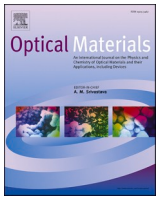
Optical Materials 149 (2024) 114801



Contents lists available at ScienceDirect

Optical Materials

journal homepage: www.elsevier.com/locate/optmat



Research Article



Biomimetic flexible SERS substrates replicated from cicada wings for portable in situ detection

Xiaojian Li [a], Hefu Li [a,*], Kai Zhao [b], Hongjun Wang [a], Zhaoyi Zhang [a], Lili Huang [a], Huijuan Niu [a], Zhenshan Yang [a], Changzheng Wang [b,**]

[a] School of Physical Science and Information Technology, Key Laboratory of Optical Communication Science and Technology of Shandong Province, Liaocheng University, Liaocheng, 252000, China
[b] School of Materials Science and Engineering, Liaocheng University, Liaocheng, 252000, China

ARTICLE INFO

Keywords:
SERS
Ag NPs
PDMS nanopore arrays
Malachite green
Portable in situ detection

ABSTRACT

Flexible surface-enhanced Raman scattering (SERS) substrate has received great attention because of its unique advantages at fast detection and on-site analysis in practical applications. Here, a biomimetic flexible SERS substrate was fabricated on polydimethylsiloxane (PDMS) film with nanopore arrays which was completely transferred from nanostructures in cicada wings by a replication process, and loaded with uniform silver nanoparticles (Ag NPs) via efficient magnetron sputtering method. By optimizing the deposition time, the optimal biomimetic flexible SERS substrate provided an analytical enhancement factor (4.2×10^5), excellent uniformity and reproducibility with a relative standard deviation (RSD) of 7.3 % and 2.8 %, respectively. Moreover, the biomimetic flexible SERS substrate exhibited excellent mechanical stability, and can obtain high-quality SERS signals under backside illumination. Specifically, malachite green (MG) residues on apple and pear peel can be rapidly and reliably determined using a portable Raman spectrometer, with a minimum detectable concentration of 10^{-6} M and a high correlation coefficient ($R^2 > 0.99$). The proposed biomimetic flexible SERS substrate coupled with a portable Raman spectrometer has great potential to be implemented in point-of-care testing applications.

1. Introduction

Surface-enhanced Raman scattering (SERS) is an attractive and powerful analytical technique, which can identify different types of analytes based on Raman spectroscopy's fingerprinting ability [1]. Due to its unique advantages of ultra-high sensitivity, rapid detection, and nondestructive analysis, SERS has been widely used in various fields, such as food safety, environmental monitoring, biomedical science, and optical anticounterfeiting [2–5]. Generally, the strong amplification of Raman signals depends on electromagnetic field enhancement at nanogaps (so-called "hot spots") among metal nanostructures due to the excitation of localized surface plasmon resonance (LSPR) [6–8]. Therefore, substantial efforts have been devoted to the fabrication of SERS substrates with high-density and uniform hot spots to meet the analytical requirements of sensitivity and reproducibility. One of the most commonly used strategy is to fabricate ordered plasmonic nanostructures on rigid substrates, which can improve SERS sensitivity and reproducibility of spectra analysis [9,10]. However, the utilization of such rigid SERS substrates for directly detecting analytes on curved surfaces is impracticable, which greatly restricts its practical applications.

Recently, flexible SERS substrates have been attracting increasing research enthusiasm. Compared to conventional rigid SERS substrates, they have distinctive advantages at convenient sampling and on-site detection of targeted analytes on irregular surfaces [11]. Many soft materials, such as paper [12], nanocellulose fibers [13], PDMS [14], and PMMA [15], have been used for constructing flexible SERS substrates. In particular, the use of flexible and transparent polymer films as templates further propelled the SERS technique into the real-world applications, as they can perform in situ and nondestructive detection of analytes via a "paste and read" strategy [16]. Especially, such SERS substrates coupled with hand-held Raman spectrometers can achieve real-time, on-site detection of analytes, bringing SERS technique closer to real-life applications [17,18]. Recently, polydimethylsiloxane (PDMS) has attracted

* Corresponding author.
** Corresponding author.
E-mail addresses: lihefu@lcu.edu.cn (H. Li), wangchangzheng@lcu.edu.cn (C. Wang).

https://doi.org/10.1016/j.optmat.2023.114801
Received 9 November 2023; Accepted 27 December 2023
Available online 22 February 2024
0925-3467/© 2023 Published by Elsevier B.V.

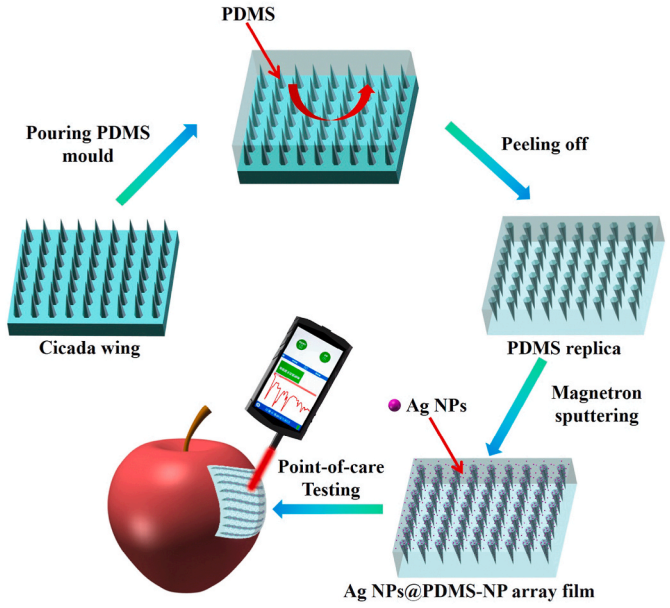


Fig. 1. Schematic illustration of the preparation process for the biomimetic flexible SERS substrate and portable in situ detection of pesticide residues in apple peel.

much attention due to its flexibility and optical transparency, which is the ideal matrix to fabricate flexible SERS substrates. Although flexible and transparent SERS substrates have many inherent advantages, the enhancement and reproducibility of the substrates are still strongly dependent on the density and uniformity of hot spots. To solve this issue, construction of three-dimensional (3D) SERS substrates prepared by decorating metallic nanostructures on periodic ordered structure arrays, has proven to be an effective way to realize highly sensitive and reproducible SERS substrates, due to their large specific area and uniformly distributed hot spots [19,20]. The simple method to fabricate PDMS film with stereoscopic array structure is to replicate patterns of template, such as silicon mold with micropatterns [21], anodic aluminum oxide [22], polystyrene spheres [23], and sapphire substrate [24]. However, the preparation process of pre-fabricated ordered patterns has high preparation cost and low output, and thus, it is still not easy to fabricate a cost-effective SERS substrate with uniformly ordered array of structures to satisfy practical applications. Thus, a few researches have utilized the molding transfer technology to transfer the surface structures of biomaterials, such lotus leaves [25,26], rose petals [27], insect wings [28,29], onto the PDMS film surfaces, and decorated metal nanoparticles to fabricate 3D SERS substrates. In particular, there are large-area nanopillars arrays on the cicada wing surface [30,31]. In addition, for in situ detection, it is necessary to make enough SERS hot spots on the film surface for better contact with the analytes on curved surfaces. Thus, a combination of cost-effective fabrication method with high-density, uniform, and accessible SERS hot spots is needed to widen the SERS technique for field analysis.

In this paper, we developed a biomimetic flexible SERS substrate composed of Ag NPs and PDMS nanopore arrays. The uniform PDMS nanopore arrays were controllably prepared by replicating ordered nanopillar arrays on cicada wing and served as a building block for deposition of Ag NPs. Using the R6G as a probe molecule, the satisfactory SERS performances of Ag NPs@PDMS nanopore array (Ag NPs@PDMS-NP array) was demonstrated by high sensitivity, excellent uniformity and batch-to-batch reproducibility, as well as good storage stability. Furthermore, the as-prepared biomimetic SERS substrate exhibited superior mechanical stability and bidirectional excitation capability, thus, it can be pasted on the irregular object surfaces and implemented back illumination to easily realize in situ SERS detection. To evaluate the suitability for field applications, the biomimetic flexible substrate combined with a portable Raman spectrometer was exploited to perform portable in situ SERS detection of malachite green (MG) residues on apple and pear peel. The minimum detection concentration as low as 10^{-6} M was achieved for both fruits. Therefore, combined with a portable Raman instrument, such biomimetic flexible SERS substrate with high performance has great potential for on-site, in situ detection applications.

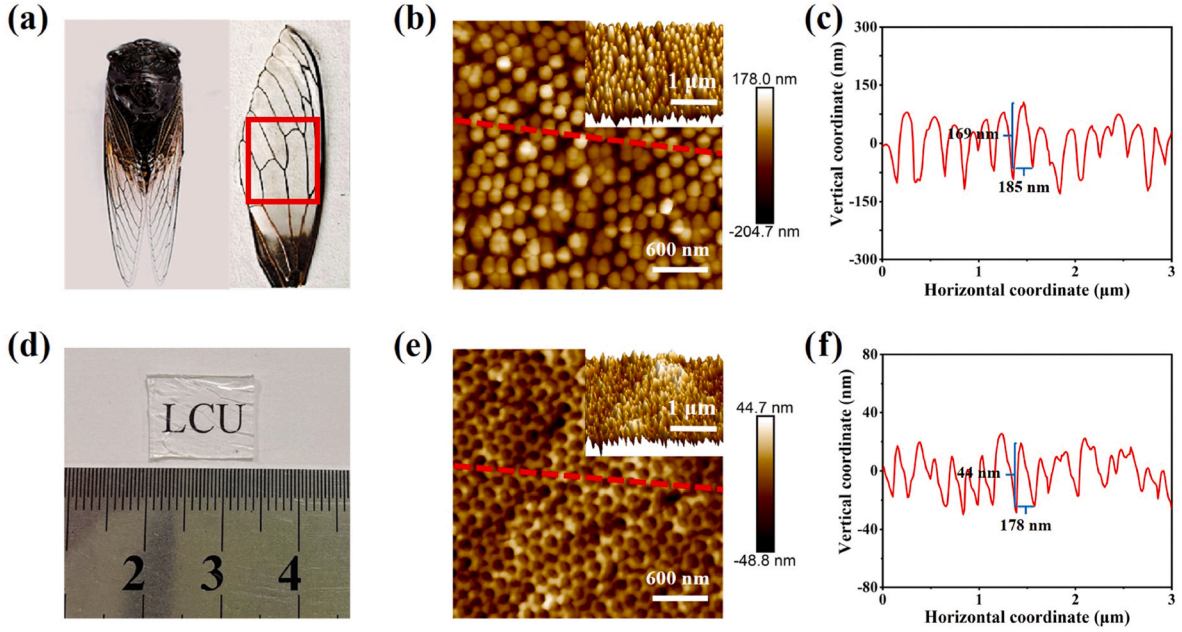


Fig. 2. (A) Photographs of a cicada and its detached forewing. (b) AFM image and (c) cross-section height profile of the cicada wing. (d) Photograph of a PDMS negative replica placed on the paper printed with letters LCU. (e) AFM image and (f) cross-section height profile of the PDMS negative replica.

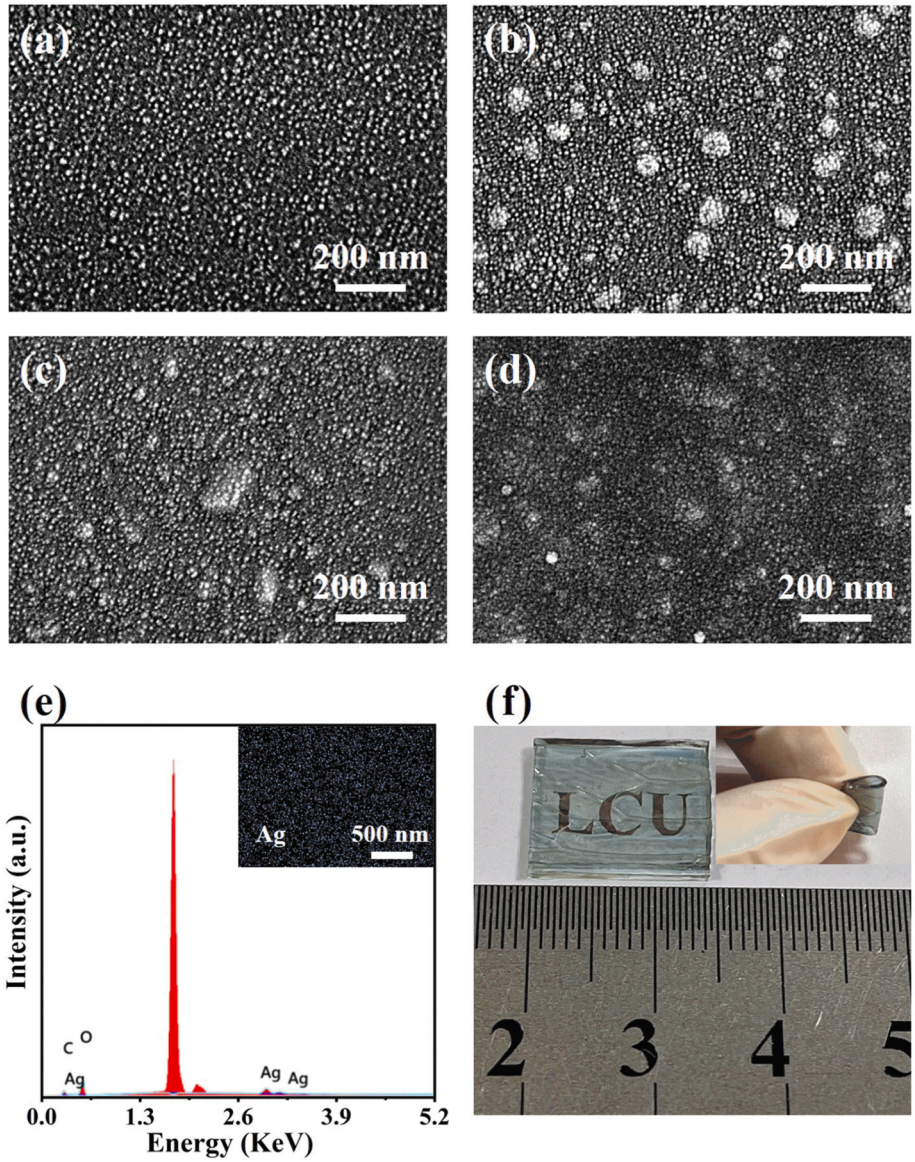


Fig. 3. SEM images of the biomimetic flexible SERS substrates prepared at different deposition times: (a) 30 s, (b) 45 s, (c) 60 s, (d) 75 s. (e) EDS spectra of the biomimetic flexible SERS substrate prepared with a deposition time of 60 s, the inset shows the Ag element distribution. (f) Photographs of a biomimetic flexible SERS substrate placed on the paper and/or folded by hand.

2. Experimental detail

2.1. Fabrication of biomimetic flexible SERS substrate

The overall fabrication process implemented to prepare the biomimetic flexible SERS substrate was depicted in Fig. 1. First, the cicada wing was ultrasonically cleaned in acetone, ethanol and ultra-pure water for 10 min, respectively, to remove surface impurities and dried with dry nitrogen. The cicada wing was then cut into 1.2 × 1.4 cm^2, and fixed on a cleaned silicon wafer using a transparent adhesive tape. Then, the mixture of PDMS prepolymer and a curing agent in a weight ratio of 10:1 (Down Corning Corp.) was dropped onto the surface of cicada wings and placed in a vacuum chamber for 30 min of degassing, followed by curing at 70 °C for 2.5 h. Subsequently, the PDMS film with ordered nanopore arrays was obtained after peeling off from the original biological template. Finally, the silver nanoparticles (Ag NPs) were deposited on the nanopatterned PDMS film through DC magnetron sputtering system to obtain the biomimetic flexible SERS substrate at different deposition times from 30 to 75 s at an interval of 15 s. During the deposition process, the DC power, base pressure, and working pressure was 20 W, 5.0 × 10^{-4} Pa, and 0.8 Pa, respectively.

2.2. Characterization and SERS measurements

The surface morphology of the cicada wings was characterized by an atomic force microscope (AFM, Bruke Icon). The morphology of the biomimetic flexible SERS substrate was investigated by a field emission scanning electron microscope (FESEM, Regulus8100, HITACHI). The SERS spectra were collected by a hand-held Raman spectrometer (TR6500, Optosky photoelectric Co., Ltd., China) equipped with a 785 nm laser source. The laser power and the accumulation time was 20 mW and 10 s, respectively. For evaluating the SERS activity of samples, 10 μL of R6G standard solutions were dripped onto the biomimetic flexible SERS substrates, and the SERS signals were collected after drying naturally. To study in situ detection capability of the SERS substrates, 20 μL of MG standard solutions were dripped onto the surface of apple and pear, and dried naturally at room temperature. Then, Ag NPs/PDMS nanopore arrays film was pasted on the contaminated apple and pear

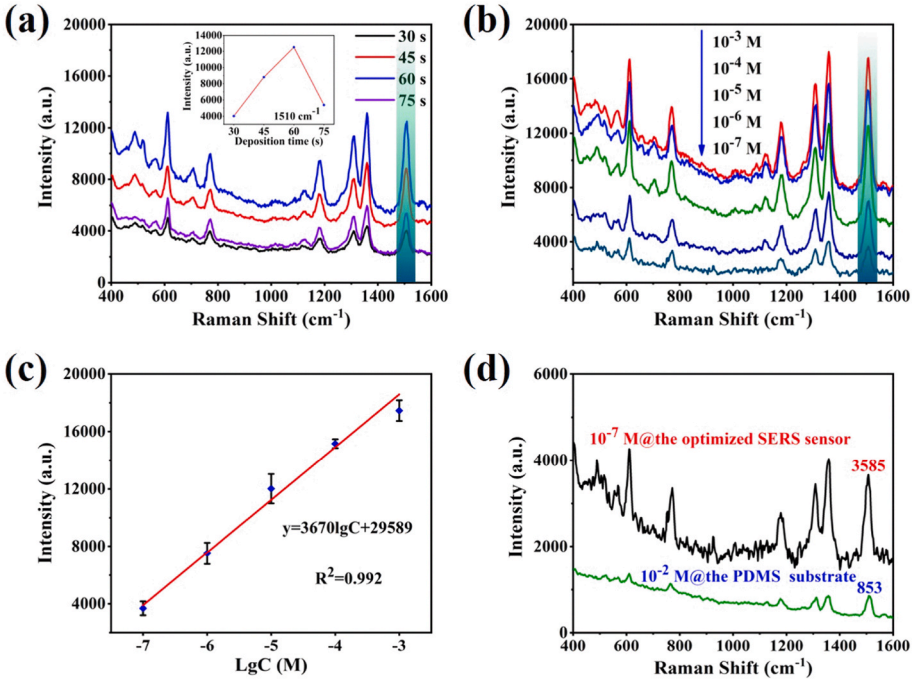


Fig. 4. (A) SERS spectra of R6G (10^{-5} M) collected from different biomimetic flexible SERS substrates. The inset shows the comparison of peak intensity at 1510 cm^{-1} for different deposition times. (b) SERS spectra of R6G with different concentrations on the optimal biomimetic flexible SERS substrate. (c) The calibration curve of the Raman intensity at 1510 cm^{-1} versus the logarithm of the R6G concentration. (d) SERS spectra of R6G (10^{-7} M) on the biomimetic flexible SERS substrate and Raman spectra of R6G (10^{-2} M) on the pure PDMS film.

with Ag NPs facing the peel surface, and performed in situ backside SERS measurements.

3. Results and discussion

Fig. 2(a) shows an image of a cicada and detached wing. According to previous reports, the cicada wing surface comprises nanopillar arrays [30,31]. As presented in Fig. 2(b), hexagonally packed nanopillar arrays are uniformly distributed on the surface of the cicada wing. The AFM analysis (Fig. 2(c)) shows that the bottom diameter and height of protrusion structure are about 185 and 169 nm, respectively. After molding, a large-area negative PDMS replica was obtained as shown in Fig. 2(d). The AFM measurement (Fig. 2(e) (f)) depicts that the negative PDMS replica consisted of ordered hexagonal close-packed nanoporous structure with a height of 44 nm and bottom diameter of 178 nm. According to these results, it can be found that the negative PDMS replica with nanoporous structures can be prepared by using cicada wings as templates.

As a mature processing technology, magnetron sputtering is an ideal method for fabricating SERS substrates because it can achieve large-scale, low-cost and time-saving deposition of thin films in a controllable manner [32,33]. The PDMS nanopore arrays decorated with Ag NPs prepared at different deposition times (from 30 to 75 s at an interval of 15 s) were characterized by SEM, as shown in Fig. 3(a)–(d). It can be seen that the size of Ag NPs can be tuned by changing the deposition time. The size of Ag NPs increased with increasing deposition time from 30 to 60 s, while the nanogaps between neighboring Ag NPs decreased. However, further increasing the Ag deposition time resulted in cluster coalescence. Thus, the Ag NPs coated PDMS nanopore arrays prepared at the deposition time of 60 s reached the optimum requirement. Moreover, energy dispersive X-ray spectroscopy (EDS) (Fig. 3(e)) reveals that the resulting biomimetic flexible substrates were mainly composed of Ag, C, and O. Also, through the EDS mapping (the inset of Fig. 3(e)), the Ag elements are found to be uniformly distributed on the surface of the biomimetic flexible substrate. Fig. 3(f) shows an image of the biomimetic flexible substrate, indicating that it has good transparency and excellent flexibility, which are verified by clear observation of letters LCU under the substrate and large bending deformation by hand.

To evaluate the SERS performance of biomimetic flexible SERS substrates, R6G with a concentration of 10^{-5} M was selected as a probe molecule. Fig. 4(a) shows the SERS spectra of R6G collected from these different biomimetic flexible SERS substrates. The major peaks of R6G in the SERS spectra were located at 612, 770, 1362, and 1510 cm^{-1}, which were similar to previous studies [34,35]. It can be seen that the SERS signals increased with increasing the deposition time to 60 s, but decreased with further elongation of the sputtering time. The SERS intensity at 1510 cm^{-1} versus the deposition time also clearly demonstrates that the substrate prepared at the deposition time of 60 s exhibits the highest Raman enhancement, as represented in the inset of Fig. 4(a). This variation of the SERS activity can be explained by the morphological evolution of the biomimetic flexible SERS substrates with different deposition times (Fig. 3(a)–(d)). For short Ag deposition time, e.g., 30 s, isolated Ag NPs with relatively small diameter was not beneficial to generate hot spots. With prolongation of the deposition time to 45 s, the size of Ag NPs on the PDMS became bigger, while interparticle nanogaps decreased, giving rise to higher SERS enhancement. With further elongation of the deposition time to 60 s, Ag NPs became bigger in size and the interparticle nanogaps became narrower, conducive to the excitation of high-density hot spots. However, when the deposition time was up to 75 s, the agglomeration of Ag NPs caused the reduction of hot spots number.

The SERS sensitivity of the optimal biomimetic flexible SERS substrate was evaluated by measuring SERS signals of R6G at different concentrations (10^{-3}-10^{-7} M), as shown in Fig. 4(b). It can be observed that a low concentration of 10^{-7} M for R6G can be readily clearly identified, indicating that this substrate has good SERS activity. Additionally, a good linear relationship between the peak intensity at 1510 cm^{-1} and the logarithmic concentration of R6G was obtained with a high correlation coefficient ($R^2 = 0.992$), as demonstrated in Fig. 4(c). Additionally, analytical enhancement factor (AEF) of the biomimetic

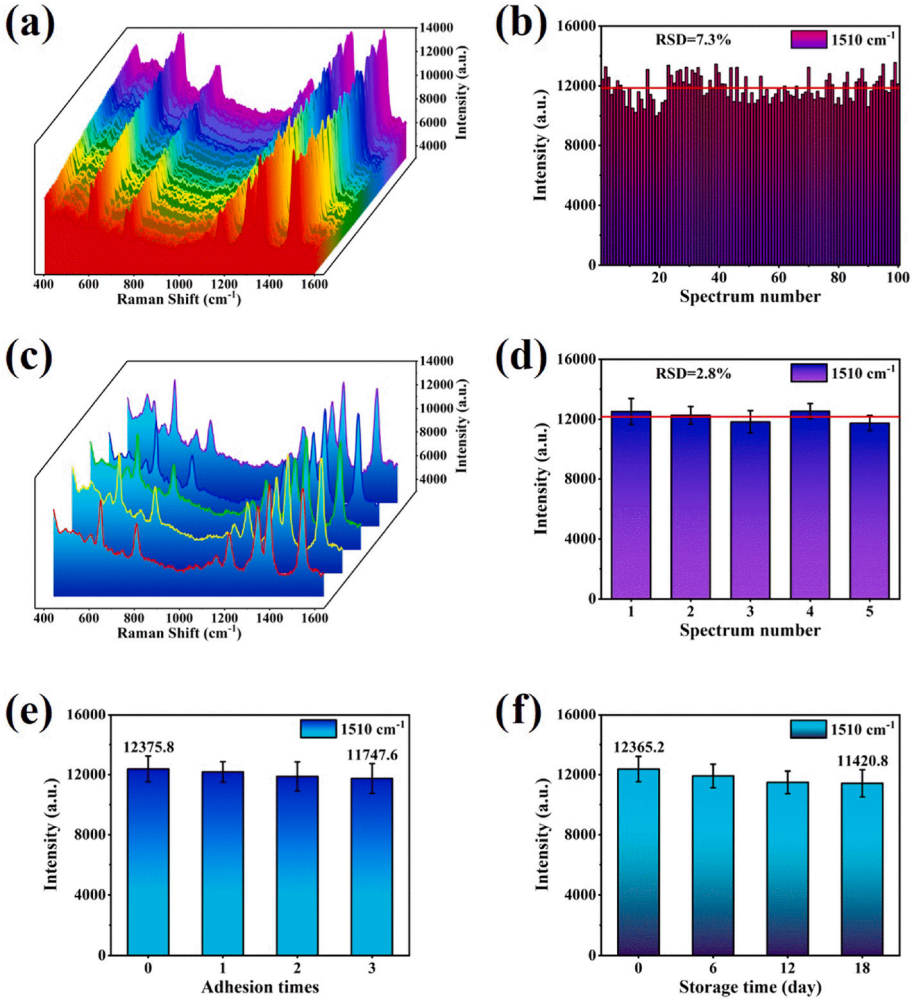


Fig. 5. (A) SERS spectra and (b) intensity distribution at 1510 cm^{-1} for 10^{-5} M R6G collected from 100 random sites on the same substrate. (c) SERS spectra and (d) intensity distribution at 1510 cm^{-1} for 10^{-5} M R6G measured from 5 batches of substrates. SERS intensity of R6G (10^{-5} M) at 1510 cm^{-1} on the biomimetic flexible SERS substrate (e) in the adhesion test and (f) stored over different periods of time.

flexible SERS substrates was calculated according to the formula [36]:

$$AEF = (I_{SERS}/C_{SERS})/(I_{NR}/C_{NR}) \quad (1)$$

Where I_{SERS} and I_{NR} are the Raman intensities of probe molecules in the SERS spectra and the norm Raman spectra. C_{SERS} and C_{NR} represent the concentration of probe molecules absorbed on the biomimetic flexible substrate and pure PDMS film, respectively. Here, the characteristic band at 1510 cm^{-1} for R6G was selected for calculation, and I_{SERS} and I_{NR} were 3585 and 853, respectively (Fig. 4(d)). The concentration of R6G used for C_{SERS} and C_{NR} was 10^{-7} M and 10^{-2} M, respectively. As a result, the AEF was calculated to be 4.2×10^5.

To access the signal uniformity, the SERS spectra of R6G (10^{-5} M) at 100 random spots on the substrate were collected, as depicted in Fig. 5 (a). The relative standard deviation (RSD) value of the peak intensity at 1510 cm^{-1} was calculated to be 7.3 % (Fig. 5(b)), confirming that the biomimetic flexible SERS substrate has excellent homogeneity. Moreover, the batch-to-batch reproducibility was evaluated by obtaining the SERS signals of R6G from 5 different biomimetic flexible SERS substrates, as shown in Fig. 5(c). The RSD value of the peak intensity at 1510 cm^{-1} was calculated to be 2.8 % (Fig. 5(d)). The excellent reproducibility can be attributed to the synergistic effect of periodic ordered PDMS nanopore arrays and homogeneous hot spots among Ag NPs, as well as reproducible fabrication process. Moreover, the adhesion test was also performed to access the robustness of Ag NPs and PDMS nanopore arrays. After three cycles of "press and peeled-off" processes using scotch tapes, the SERS intensity at peak 1510 cm^{-1} did not change significantly and decreased by about 5 %, as shown in Fig. 5(e), indicating that Ag NPs had strong adhesion on the PDMS film surface. Also, the stability of the biomimetic flexible SERS substrate was tested under ambient environment storage conditions. As shown in Fig. 5(f), the peak intensity at 1510 cm^{-1} recorded from the SERS substrate stored for 18 days attenuates by 8 % compared with the fresh substrate, showing that the biomimetic substrate exhibits good time stability.

To effectively achieve in situ detection of contaminants on curved surfaces, the SERS substrate must have excellent mechanical stability and superior bidirectional detection capability. Towards this end, the service properties of the biomimetic flexible SERS substrates were investigated by subjecting to a series of fatigue tests, including bending, torsion, and stretching, as shown in the inset of Fig. 6(a)–(c). For the bending, torsion, and stretching test, the obtained SERS substrates were bent in half, twisted to ~180° and stretched to ~150 %, respectively. The SERS signals were collected from R6G (10^{-5} M) molecules absorbed on the biomimetic flexible SERS substrate after every ten deformation operations. After 100 bending, torsion and stretching cycles, the peak intensity at 1510 cm^{-1} hardly changes compared to the original value before deformations, as shown in Fig. 6(a)–(c), indicating that the biomimetic flexible SERS substrate has excellent mechanical property and adaptability. Furthermore, as the obtained biomimetic flexible SERS substrate has excellent optical transparency (Fig. 3(f)), we collected the SERS spectra of MG at different concentrations from both sides of the as-

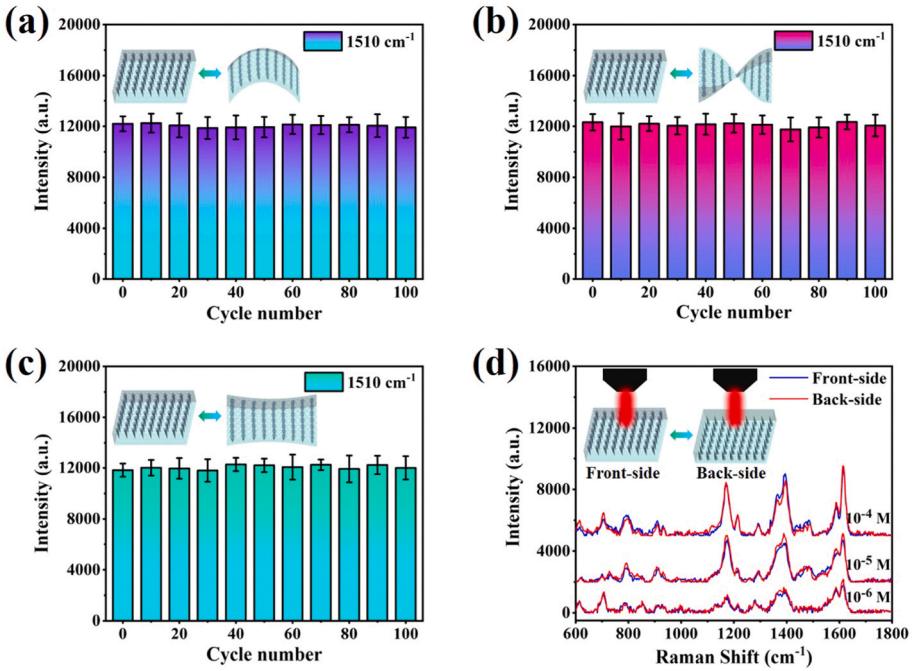


Fig. 6. SERS intensity of R6G collected from the biomimetic flexible SERS substrate during the (a) bending, (b) torsion, and (c) stretching tests for 100 cycles. (d) SERS spectra of MG at different concentrations collected from both sides of the biomimetic flexible SERS substrate.

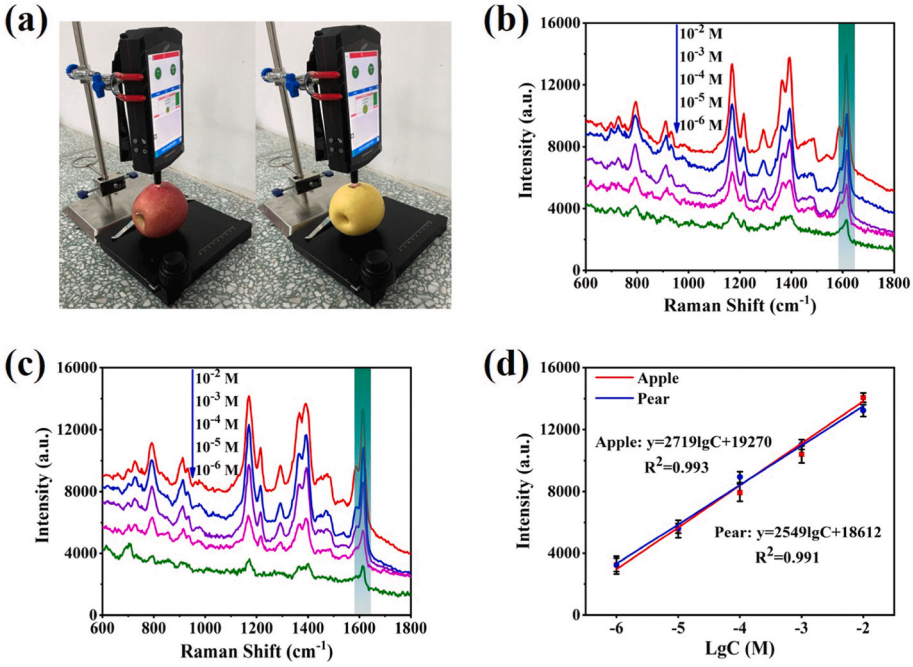


Fig. 7. (A) Portable in situ SERS detection measurement on apple and pear peel. SERS spectra of MG with different concentrations collected from the surface of (b) apple peel, and (c) pear peel using the biomimetic flexible SERS substrate. (d) Linear calibration plot between the SERS intensity at 1616 cm^{-1} and logarithm of MG concentration (red, apple; blue, pear).

prepared substrate, as shown in Fig. 6(d). It was found that the obtained SERS signal were almost identical, suggesting that the biomimetic flexible SERS substrate could be used for in situ analysis by the backside SERS measurement. These results demonstrated the excellent mechanical stability and good bidirectional excitation property of the biomimetic flexible SERS substrate, which would be useful for in situ detection of analytes on irregular surfaces.

To investigate the applicability of the biomimetic flexible SERS substrate for real-world applications, MG was selected as the model analyte [37,38]. For portable in situ SERS detection, the biomimetic flexible SERS substrates were pasted on apple and pear peel, which were spiked with MG at different concentrations, and the SERS signals were collected under backside illumination mode by means of a hand-hold Raman spectrometer, as shown in Fig. 7(a). The SERS spectra of MG with different concentrations on apple and pear peels collected by biomimetic flexible SERS substrates are shown in Fig. 7(b), (c),

respectively. It was found that a low MG concentration of 10^{-6} M can be readily detected via a portable Raman spectrometer. In addition, there is a good linear relationship between the peak intensity at 1616 cm^{-1} and the logarithm of MG concentration for two types of fruit with R^2 of 0.993 and 0.991, respectively. The above results indicated that the biomimetic flexible SERS substrate could be used for realizing simple, rapid, and on-site detection applications using a portable Raman spectrometer.

4. Conclusion

In conclusion, we fabricated a biomimetic flexible SERS substrate and explored its applications for on-site, in situ hazardous residues detection in fruits. The PDMS film with ordered nanopore arrays was prepared by replicating nanochitin in the cicada wings, and served as a patterned template for Ag NPs deposition. Since the combination of high-density hot spots and periodic order nanopore array, the optimal biomimetic flexible SERS substrate exhibited high AEF (4.2×10^5), excellent signal uniformity (RSD = 7.3 %), and superior batch-to-batch reproducibility (RSD = 2.8 %). In additions, it also had excellent mechanical stability and SERS enhancement under backside illumination mode. Combined with a hand-hold Raman spectrometer, the rapid, on-site, and in situ MG residues detection on apple or pear peel can be readily performed using the biomimetic flexible substrate. The minimum detection concentration of MG for both fruits was 10^{-6} M, and the SERS intensity and the logarithmic concentration exhibited a good linear relationship ($R^2 > 0.99$). These results indicated that the as-prepared biomimetic flexible SERS substrate coupled with a portable Raman spectrometer has broad application potential for rapid, on-site detection of contaminants on irregular surfaces.

CRediT authorship contribution statement

Xiaojian Li:Methodology, Resources, Investigation, Formal analysis. **Hefu Li:** Investigation, Writing – original draft, Formal analysis, Supervision, Funding acquisition. **Kai Zhao:** Methodology, Resources, Investigation. **Hongjun Wang:** Resources, Visualization. **Zhaoyi Zhang:** Data curation. **Lili Huang:** Investigation, Visualization. **Huijuan Niu:** Formal analysis, Funding acquisition. **Zhenshan Yang:** Writing – review & editing. **Changzheng Wang:** Conceptualization, methodology, validation, Supervision.

Declaration of competing interest

The authors declare that they have no known competing financial interests or personal relationships that could have appeared to influence the work reported in this paper.

Data availability

Data will be made available on request.

Acknowledgements

This work was supported by Natural Science Foundation of Shandong Province (grant numbers ZR2021MF097, ZR2022MF305); Liaocheng University Start-up Fund for Doctoral Scientific Research (grant number 318051542).

References

[1] S.Y. Ding, J. Yi, J.F. Li, B. Ren, D. Wu, R. Panneerselvam, Z.Q. Tian, Nanostructure-based plasmon-enhanced Raman spectroscopy for surface analysis of materials, Nat. Rev. Mater. 1 (2016) 16021.
[2] L. Jiang, M.M. Hassan, S. Ali, H. Li, R. Sheng, Q. Chen, Evolving trends in SERS-based techniques for food quality and safety: a review, Trends Food Sci. Technol. 112 (2021) 225–240.
[3] S.W. Cho, H. Wei, Surface-enhanced Raman spectroscopy for emerging contaminant analysis in drinking water, Front. Environ. Sci. Eng. 17 (2023) 57.
[4] Q. Li, H. Huo, Y. Wu, L. Chen, L. Su, X. Zhang, J. Song, H. Yang, Design and synthesis of SERS materials for in vivo molecular imaging and biosensing, Adv. Sci. 10 (2023) 2202051.
[5] Y. Sun, D. Lou, W. Liu, Z. Zheng, X. Chen, SERS labels for optical anticounterfeiting: structure, fabrication, and performance, Adv. Opt. Mater. 11 (2023) 2201549.
[6] K. Kneipp, Y. Wang, H. Kneipp, L.T. Perelman, I. Itzkan, R.R. Dasari, M.S. Feld, Single molecule detection using surface-enhanced Raman scattering (SERS), Phys. Rev. Lett. 78 (1997) 1667–1670.
[7] L. Tian, C. Wang, H. Zhao, F. Sun, H. Dong, K. Feng, P. Wang, G. He, G. Li, Rational approach to plasmonic dimers with controlled gap distance, symmetry, and capability of precisely hosting guest molecules in hotspot regions, J. Am. Chem. Soc. 143 (2021) 8631–8638.
[8] S. Schlücker, Surface-enhanced Raman spectroscopy: concepts and chemical applications, Angew. Chem. Int. Ed. 53 (2014) 4756–4795.
[9] B.C. Galarreta, P.R. Norton, F. Lagugne-Labarthet, SERS detection of streptavidin/biotin monolayer assemblies, Langmuir 27 (2011) 1494–1498.
[10] J. Huang, F. Chen, Q. Zhang, Y. Zhan, D. Ma, K. Xu, Y. Zhao, 3D Silver nanoparticles decorated zinc oxide/silicon heterostructured nanomace arrays as high-performance surface-enhanced Raman scattering substrates, ACS Appl. Mater. Interfaces 7 (2015) 5725–5735.
[11] L. Xie, H. Zeng, J. Zhu, Z. Zhang, H.B. Sun, W. Xia, Y. Du, State of the art in flexible SERS sensors toward label-free and onsite detection: from design to applications, Nano Res. 15 (2022) 4374–4394.
[12] H. Torul, H. Çiftçi, D. Çetin, Z. Suludere, I.H. Boyacl, U. Tamer, Paper membrane-based SERS platform for the determination of glucose in blood samples, Anal. Bioanal. Chem. 407 (2015) 8243–8251.
[13] J. Chen, M. Huang, L. Kong, Flexible Ag/nanocellulose fibers SERS substrate and its applications for in-situ hazardous residues detection on food, Appl. Surf. Sci. 533 (2020) 147454.
[14] L. Li, W.S. Chin, Rapid fabrication of a flexible and transparent Ag nanocubes@PDMS film as a SERS substrate with high performance, ACS Appl. Mater. Interfaces 12 (2020) 37538–37548.
[15] L.B. Zhong, J. Yin, Y.M. Zheng, Q. Liu, X.X. Cheng, F.H. Luo, Self-assembly of Au nanoparticles on PMMA template as flexible, transparent, and highly active SERS substrates, Anal. Chem. 86 (2014) 6262–6267.
[16] Z. Li, X. Huang, G. Lu, Recent developments of flexible and transparent SERS substrates, J. Mater. Chem. C 8 (2020) 3956–3969.
[17] K. Xu, R. Zhou, K. Takei, M. Hong, Toward flexible surface-enhanced Raman scattering (SERS) sensors for point-of-care diagnostics, Adv. Sci. 6 (2019) 1900925.
[18] W. Hu, L. Xia, Y. Hu, G. Li, Recent progress on three-dimensional substrates for surface-enhanced Raman spectroscopic analysis, Microchem. J. 172 (2022) 106908.
[19] H. Zhang, N. Zhao, H. Li, M. Wang, X. Hao, M. Sun, X. Li, Z. Yang, H. Yu, C. Tian, C. Wang, 3D flexible SERS substrates integrated with a Portable Raman analyzer and wireless communication for point-of-care application, ACS Appl. Mater. Interfaces 14 (2022) 51253–51264.
[20] Z. Huang, G. Meng, Q. Huang, Y. Yang, C. Zhu, C. Tang, Improved SERS performance from Au nanopillar arrays by abridging the pillar tip spacing by Ag sputtering, Adv. Mater. 22 (2010) 4136–4139.
[21] R. Gao, H. Qian, C. Weng, X. Wang, C. Xie, K. Guo, S. Zhang, S. Xuan, Z. Guo, L. B. Luo, A SERS stamp: multiscale coupling effect of silver nanoparticles and highly ordered nano-micro hierarchical substrates for ultrasensitive explosive detection, Sens. Actuators B: Chem. 321 (2020) 128543.
[22] P. Wang, L. Wu, Z. Lu, Q. Li, W. Yin, F. Ding, H. Han, Gecko-inspired nanotentacle surface-enhanced Raman spectroscopy substrate for sampling and reliable detection of pesticide residues in fruits and vegetables, Anal. Chem. 89 (2017) 2424–2431.
[23] C.T. Mallon, K.W. Kho, H. Gartite, R.J. Forster, T.E. Keyes, Fabrication and optical properties of periodic Ag nano-pore and nano-particle arrays with controlled shape and size over macroscopic length scales, Adv. Eng. Mater. 20 (2018) 1700532.
[24] L. Zhang, X. Li, W. Liu, R. Hao, H. Jia, Y. Dai, M.U. Amin, H. You, T. Li, J. Fang, Highly active Au NP microarray films for direct SERS detection, J. Mater. Chem. C 7 (2019) 15259–15268.
[25] P. Kumar, R. Khosla, M. Soni, D. Deva, S.K. Sharma, A highly sensitive, flexible SERS sensor for malachite green detection based on Ag decorated microstructured PDMS substrate fabricated from Taro leaf as template, Sens. Actuators B: Chem. 246 (2017) 477–486.
[26] Z. Zhu, X. Shi, Y. Feng, M. He, C. Ye, H. Zhou, M. Zhang, W. Zhang, J. Li, C. Jiang, Lotus leaf mastoid inspired Ag micro/nanoarrays on PDMS film as flexible SERS sensor for in-situ analysis of pesticide residues on nonplanar surfaces, Spectrochim. Acta Mol. Biomol. Spectrosc. 288 (2023) 122211.
[27] U.T. Pham, Q.H.T. Phan, L.P. Nguyen, P.D. Luu, T.D. Doan, H.T. Trinh, C.T. Dinh, T.V. Nguyen, T.Q. Tran, D.X. Le, T.N. Pham, T.D. Le, D.T. Nguyen, Rapid quantitative determination of multiple pesticide residues in mango fruits by surface-enhanced Raman spectroscopy, Processes 10 (2022) 442.
[28] C.H. Lu, M.R. Cheng, S. Chen, W.L. Syu, M.Y. Chien, K.S. Wang, J.S. Chen, P.H. Lee, T.Y. Liu, Flexible PDMS-based SERS substrates replicated from beetle wings for water pollutant detection, Polymers 15 (2023) 191.
[29] X. Yan, H. Shi, P. Jia, X. Sun, LSPR tunable Ag@PDMS SERS substrate for high sensitivity and uniformity detection of dye molecules, Nanomaterials 12 (2022) 3894.
[30] S. Xiang, C. Ge, S. Li, L. Chen, L. Wang, Y. Xu, In situ detection of endotoxin in bacteriostatic process by SERS chip integrated array microchambers within

bioscaffold nanostructures and SERS tags, ACS Appl. Mater. Interfaces 12 (2020) 28985–28992.
[31] F. Shao, Z. Lu, C. Liu, H. Han, K. Chen, W. Li, Q. He, H. Peng, J. Chen, Hierarchical nanogaps within bioscaffold arrays as a high-performance SERS substrate for animal virus biosensing, ACS Appl. Mater. Interfaces 6 (2014) 6281–6289.
[32] W. Gao, J. Xu, C. Cheng, S. Qiu, S. Jiang, Rapid and highly sensitive SERS detection of fungicide based on flexible "wash free" metallic textile, Appl. Surf. Sci. 512 (2020) 144693.
[33] J. Cai, Z. Wang, M. Wang, D. Zhang, Au nanoparticle-grafted hierarchical pillars array replicated from diatom as reliable SERS substrates, Appl. Surf. Sci. 541 (2021) 148374.
[34] C. Byram, S.S.B. Moram, V.R. Soma, SERS based detection of multiple analytes from dye/explosive mixtures using picosecond laser fabricated gold nanoparticles and nanostructures, Analyst 144 (2019) 2327–2336.
[35] Y. Li, J. Li, T. Wang, Z. Zhang, Y. Bai, C. Hao, C. Feng, Y. Ma, R. Sun, Facile fabrication of superhydrophobic hybrid nanotip and nanopore arrays as surface-enhanced Raman spectroscopy substrates, Appl. Surf. Sci. 443 (2018) 138–144.
[36] E.C.L. Ru, E. Blackie, M. Meyer, P.G. Etchegoin, Surface enhanced Raman scattering enhancement factors: a comprehensive study, J. Phys. Chem. C 111 (2007) 13794–13803.
[37] X. Tian, Q. Fan, J. Guo, Q. Yu, L. Xu, X. Kong, Surface-enhanced Raman scattering of flexible cotton fiber-Ag for rapid adsorption and detection of malachite green in fish, Spectrochim. Acta Mol. Biomol. Spectrosc. 263 (2021) 120174.
[38] Y. Chen, Q. Chen, X. Wei, Separable surface enhanced Raman spectroscopy sensor platformed by HPTLC for facile screening of malachite green in fish, Microchem. J. 170 (2021) 106694.